

## Search for Squaraine Derivatives That Can Be Sublimed without Thermal Decomposition

Minquan Tian,<sup>\*,†</sup> Makoto Furuki,<sup>†</sup> Izumi Iwasa,<sup>†</sup> Yasuhiro Sato,<sup>†</sup> Lyong Sun Pu,<sup>†</sup> and Satoshi Tatsuura<sup>‡</sup>

Corporate Research Center, Fuji Xerox Co., Ltd., 430 Sakai, Nakai-machi, Ashigarakami-gun, Kanagawa 259-0157, Japan, and The Femtosecond Technology Research Association, 5-5 Tokodai, Tsukuba, Ibaraki 300-2635, Japan

Received: October 3, 2001; In Final Form: February 18, 2002

To search for sublimable squaraine (SQ) dyes for fabricating thin films under vacuum, we have synthesized a series of 2,4-bis[4-(*N,N*-dialkylamino)-2,6-dihydroxyphenyl]squaraines [SQ(OH)<sub>4</sub>] and studied their properties. The investigation of the behavior of their Langmuir films at the air–water interface revealed that SQ(OH)<sub>4</sub> molecules with branched *N*-alkyl groups such as *sec*-butyls and isobutyls have larger limiting areas and tend to form J-aggregates in the monolayers, whereas molecules with straight *N*-alkyl chains have smaller limiting areas and are apt to form H-aggregates. This behavior is attributable to the much larger steric hindrance of the branched *N*-butyl groups than that of the straight ones. The thermal stability of these dyes was investigated by differential thermal analysis (DTA) and thermogravimetry (TG), and their sublimation ability was evaluated through heating under vacuum. As a result, we verified that the four hydroxyls at the 2',6'-positions of the two phenyl rings significantly enhanced the thermal stability and the sublimation ability of anilino SQ dye molecule, and the introduction of branched *N*-butyls further promoted the sublimation ability of the target SQ(OH)<sub>4</sub> molecules. These phenomena may be attributed to the intramolecular hydrogen bonding between the hydroxyls and the CO groups of the four-membered ring, and the much larger intermolecular repulsive force between branched *N*-alkyls, respectively. In particular, the SQ(OH)<sub>4</sub> dye with four *N*-isobutyls could be sublimed without any decomposition. These results suggest that SQ(OH)<sub>4</sub> molecule with branched *N*-butyls is the most effective structure for realizing a high sublimation ability. Furthermore, pure SQ dye thin films have been successfully fabricated by molecular beam deposition of the SQ(OH)<sub>4</sub> dye with four *N*-isobutyls. The vacuum-deposited thin films of such SQ dyes have potential applications in various fields such as electrophotography, solar energy conversion, optical recording, and nonlinear optics.

## 1. Introduction

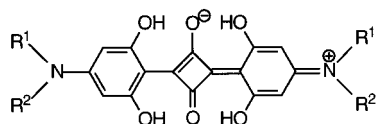
Squaraine (SQ) dyes are expected to have significant technological applications in many areas such as electrophotography,<sup>1–3</sup> solar energy conversion,<sup>4–7</sup> optical recording,<sup>8–10</sup> nonlinear optics,<sup>11–17</sup> and electroluminescence.<sup>18,19</sup> For practical application, the fabrication of thin films with high uniformity is strongly required. Although there have been a large number of reports on SQ thin films fabricated by solution-coating techniques such as Langmuir and Langmuir–Blodgett (LB) methods,<sup>15,16,20–27</sup> dip and bar coating,<sup>28–30</sup> or casting and spin coating,<sup>5,6,8,26,27,31,32</sup> several fatal limitations of the solution-coating method cannot be easily overcome. First, SQ thin films prepared by solution coating usually do not have a smooth surface, which is very important for the optical application of SQ dyes. Second, the thickness homogeneity of SQ thin films prepared by solution coating is poor. Moreover, the desired thickness of SQ thin films is difficult to control by solution coating. These limitations may be overcome by the vacuum-deposition method, because dye molecules may be evaporated very slowly and deposited onto the substrate one by one in ultrahigh vacuum. Nevertheless, only a few reports on vacuum-deposited films of SQ dyes can be found in the literature, and

the SQ materials employed for fabricating vacuum-deposited films were mainly 2,4-bis[4-(*N,N*-dialkylamino)-2-hydroxyphenyl]squaraines [SQ(OH)<sub>2</sub>],<sup>4–6,8,10</sup> 2,4-bis[4-(*N,N*-dimethylamino)-2-methylphenyl]squaraine,<sup>5,8,10</sup> and 2,4-bis[4-(*N,N*-dimethylamino)phenyl]squaraine (SQ11).<sup>8,10</sup> To fabricate SQ thin films with high uniformity for nonlinear optics, we repeated the preparation of vacuum-deposited films from the above-mentioned SQ materials. As a result, we found that pure vacuum-deposited films could not be obtained using these known SQ materials, because their thermal decomposition occurred during the process of sublimation. Moreover, we also noted that SQ(OH)<sub>2</sub> showed better thermal stability and higher sublimation ability than the corresponding analogues without any hydroxyl. For example, the thermal decomposition temperatures for SQ11 and 2,4-bis[4-(*N,N*-dimethylamino)-2-hydroxyphenyl]squaraine [SQ11(OH)<sub>2</sub>], which were obtained by TG, were 277 and 326 °C, respectively. However, we observed that SQ11 was initially sublimed at 200 °C and decomposed at 220 °C in a vacuum of  $(0.4–1) \times 10^{-3}$  Pa, whereas SQ11(OH)<sub>2</sub> was initially sublimed at 230 °C and decomposed at 260 °C in the same vacuum system. Moreover, SQ11 was found to be sublimed less easily and to decompose more easily than SQ11(OH)<sub>2</sub> in the sublimation experiments. Intramolecular hydrogen bonding between the hydroxyls and the CO groups of the four-membered ring may be the reason for this behavior. Thus, we think an anilino SQ dye molecule with four hydroxyls at the 2',6'-positions of the two phenyl rings will show even better thermal stability and

\* Telephone: +81-465-80-2276. Fax: +81-465-81-8997. E-mail: Tian.Minquan@fujixerox.co.jp.

<sup>†</sup> Fuji Xerox Co., Ltd.

<sup>‡</sup> The Femtosecond Technology Research Association.



- 1  $R^1 = R^2 = C_2H_5$
- 2  $R^1 = R^2 = n-C_3H_7$
- 3  $R^1 = n-C_3H_7, R^2 = C_2H_5(CH_3)CH$
- 4  $R^1 = R^2 = (CH_3)_2CHCH_2$
- 5  $R^1 = R^2 = n-C_4H_9$
- 6  $R^1 = R^2 = n-C_5H_{11}$
- 7  $R^1 = R^2 = n-C_6H_{13}$

Figure 1. Molecular structure of the SQ derivatives synthesized.

higher sublimation ability and may be well sublimed without any thermal decomposition.

On the other hand, some derivatives of SQ(OH)<sub>4</sub>, such as the *N,N*-dimethyl,<sup>14,33,34</sup> *N,N*-di-*n*-butyl,<sup>14,35–40</sup> *N,N*-di-*n*-pentyl,<sup>35–37,41–44</sup> *N,N*-di-*n*-hexyl,<sup>14,35–37,41–45</sup> *N*-methyl-*N*-alkyl,<sup>27,46</sup> and *N,N*-bis(2-*n*-hexyloctyl) analogues,<sup>47</sup> have been prepared, and their xerographic and nonlinear optical properties in solution-coated films or in solution have also been investigated. Moreover, Dirk et al. reported that the melting point of the *N,N*-di-*n*-butyl derivative of SQ(OH)<sub>4</sub> was higher by 45 °C than that of the corresponding SQ(OH)<sub>2</sub> analogue.<sup>14</sup> This result suggests that SQ(OH)<sub>4</sub> dyes should have better thermal stability and higher sublimation ability than the corresponding SQ(OH)<sub>2</sub> analogues. However, no information about the sublimation ability of SQ(OH)<sub>4</sub> dyes has been reported thus far.

In order for an anilino SQ dye to be sublimable, we think that the single SQ molecule should be thermally stable. Moreover, the interactions between molecules of such an SQ dye should be sufficiently small for the molecules to be evaporated in a vacuum. Therefore, the substituents that can improve the thermal stability and reduce the intermolecular interactions of an anilino SQ dye are favorable for its sublimation ability.

With such knowledge in mind, we designed and synthesized a series of SQ(OH)<sub>4</sub> derivatives (Figure 1), to find the most effective molecular structure for thin-film fabrication under vacuum. There are several reasons for such a molecular design. First, the introduction of four hydroxyls at the 2',6'-positions of the two phenyl rings may enhance the thermal stability of the target SQ dyes to such an extent that they could be sublimed without any thermal decomposition. Second, *N*-alkyl chains were varied to control intermolecular interactions so that the most effective molecular structure for high sublimation ability could be picked out. In particular, branched *N*-alkyl chains such as isobutyls and *sec*-butyls, which exhibit larger steric hindrance effects, may suppress the intermolecular hydrogen bonding between the hydroxyls and further promote the sublimation ability of the target SQ materials. In addition, the synthetic feasibility was also considered in the design of such SQ dye molecules.

In this paper, we report the synthesis, thermal stability, and sublimation ability of these SQ derivatives. The behavior of their Langmuir films at the air–water interface was also investigated in order to understand their intermolecular interactions in the solid phase. Consequently, we found the most effective structure of SQ molecules for realizing a high sublimation ability. Furthermore, pure SQ thin films were fabricated by the molecular beam deposition of those sublimable SQ dyes.

## 2. Experimental Section

**2.1. General Techniques.** IR spectra were recorded on a JASCO FTIR-23 Fourier transform infrared spectrometer, using potassium bromide pellets. <sup>1</sup>H NMR spectra with tetramethylsilane as the internal standard were recorded on a JEOL JNM-AL400 Fourier transform nuclear magnetic resonance spectrometer (400 MHz). Electron ionization (EI) mass spectra were recorded on a Shimadzu QP-5000 mass spectrometer. UV–visible absorption spectra were measured on a Hitachi U-4100 spectrophotometer in a quartz cell of path length 10 mm. Reagent chemicals and solvents were used as purchased without further purification.

**2.2. Materials.** SQ dyes 1–7 were synthesized by a modification of the reference method.<sup>14</sup> 5-*N,N*-Dialkylamino-1,3-dihydroxybenzene was prepared by the nucleophilic substitution of phloroglucinol with a secondary amine in a toluene-1-butanol solvent system under reflux with azeotropic distillation of water. The condensation of 5-*N,N*-Dialkylamino-1,3-dihydroxybenzene and squaric acid in the toluene-1-butanol solvent system under azeotropic reflux produced the desired SQ dye.<sup>47,48</sup> For the preparation of dyes 1 and 5–7, a one-pot reaction procedure similar to the reference method was used; i.e., the corresponding intermediate anilines were condensed with squaric acid without any separation. However, for the preparation of dyes 2–4, the corresponding intermediate anilines were separated and purified before condensation with squaric acid. The latter modified method gave a better yield of the desired SQ dye and is more valid for the preparation of SQ dyes with branched *N*-alkyls. New compounds 1–4 were synthesized for the first time. A representative procedure for the synthesis of this class of SQ dyes is described as follows.

**2,4-Bis[4-(*N-sec*-butyl-*N-n*-propylamino)-2,6-dihydroxyphenyl]squaraine (3).** Under dry nitrogen atmosphere, a mixture of 1,3,5-trihydroxybenzene (7.92 g, 62.8 mmol), *N-sec*-butyl-*n*-propylamine (14.48 g, 125.7 mmol), 1-butanol (50 mL), and toluene (150 mL) was refluxed for 6 h with azeotropic distillation of water. The pale-brown solution was then cooled, and the solvents were evaporated under reduced pressure to give a brown liquid. The resulting crude product was purified by column chromatography on silica gel with *n*-hexane/acetone (volume ratio 4:1 ~ 3:2) as the eluents to give a pale brown-yellow viscous liquid of 5-*N-sec*-butyl-*N-n*-propylamino-1,3-dihydroxybenzene, 4.61 g (32.9%). Then, a mixture of this aniline intermediate (4.47 g, 20 mmol), squaric acid (1.14 g, 10 mmol), 1-butanol (40 mL), and toluene (120 mL) was stirred under dry nitrogen atmosphere and refluxed for 5 h with azeotropic distillation of water. After toluene was distilled, 1-butanol was removed by azeotropic distillation with cyclohexane (70 mL). The final cyclohexane solution of approximately 15 mL was cooled, and the black-green precipitate was filtered and washed with *n*-hexane and methanol. Yellow-green crystals were recrystallized from dichloromethane-methanol to give shining yellow-green needle microcrystals, 4.16 g (79.3%). Total yield: 26.1%. IR:  $\nu_{\max}$  3430, 3087, 2965, 2925, 2870, 2695, 1625 (C=O), 1552, 1516, 1431, 1397, 1328 (C–N), 1285, 1251 (OH), 1160, 1119, 1057, 989, 965, 902, 867, 819, 796, 735 cm<sup>-1</sup>. <sup>1</sup>H NMR (CDCl<sub>3</sub>):  $\delta$  10.941 (s, 4H, OH), 5.861 (s, 4H, H<sub>arom</sub>), 3.946 (m, 2H, NCH), 3.172 (m, 4H, NCH<sub>2</sub>), 1.728~1.606 (m, 8H, CH<sub>2</sub>), 1.234 (d, *J* = 6.59 Hz, 6H, NCCH<sub>3</sub>), 0.952 (t, *J* = 7.32 Hz, 6H, CH<sub>3</sub>), 0.893 (t, *J* = 7.32 Hz, 6H, CH<sub>3</sub>). MS (EI): *m/z* 524 (M<sup>+</sup>, 50%), 495 (M<sup>+</sup>–C<sub>2</sub>H<sub>5</sub>, 100%). Anal. Calcd for C<sub>30</sub>H<sub>40</sub>O<sub>6</sub>N<sub>2</sub> (524.65): C, 68.7; H, 7.68; N, 5.34. Found: C, 67.2; H, 7.55; N, 5.18.

**2,4-Bis[4-(*N,N*-diethylamino)-2,6-dihydroxyphenyl]squaraine (1).** Shining green microcrystals, total yield: 20.0%. IR:  $\nu_{\max}$  3418, 3087, 2980, 2929, 2702, 1627 (C=O), 1565, 1528, 1432, 1402, 1329 (C–N), 1266 (OH), 1165, 1134, 1118, 1077, 981, 845, 793, 780, 733  $\text{cm}^{-1}$ .  $^1\text{H}$  NMR ( $\text{CDCl}_3$ ):  $\delta$  10.986 (s, 4H, OH), 5.807 (s, 4H,  $\text{H}_{\text{arom}}$ ), 3.431 (q,  $J = 7.08$  Hz, 8H,  $\text{NCH}_2$ ), 1.243 (t,  $J = 7.08$  Hz, 12H,  $\text{CH}_3$ ). MS (EI):  $m/z$  440 ( $\text{M}^+$ , 100%), 425 ( $\text{M}^+ - \text{CH}_3$ , 45.5%). Anal. Calcd for  $\text{C}_{24}\text{H}_{28}\text{O}_6\text{N}_2$  (440.49): C, 65.4; H, 6.41; N, 6.36. Found: C, 64.1; H, 6.19; N, 6.22.

**2,4-Bis[4-(*N,N*-dipropylamino)-2,6-dihydroxyphenyl]squaraine (2).** Shining blue-green needle microcrystals, total yield: 25.5%. IR:  $\nu_{\max}$  3422, 3087, 2964, 2929, 2877, 2695, 1626 (C=O), 1559, 1433, 1410, 1329 (C–N), 1298, 1251 (OH), 1164, 1133, 1093, 919, 867, 819, 795, 733  $\text{cm}^{-1}$ .  $^1\text{H}$  NMR ( $\text{CDCl}_3$ ):  $\delta$  10.974 (s, 4H, OH), 5.781 (s, 4H,  $\text{H}_{\text{arom}}$ ), 3.307 (t,  $J = 7.81$  Hz, 8H,  $\text{NCH}_2$ ), 1.670 (m, 8H,  $\text{CH}_2$ ), 0.953 (t,  $J = 7.57$  Hz, 12H,  $\text{CH}_3$ ). MS (EI):  $m/z$  496 ( $\text{M}^+$ , 95.6%), 467 ( $\text{M}^+ - \text{C}_2\text{H}_5$ , 100%). Anal. Calcd for  $\text{C}_{28}\text{H}_{36}\text{O}_6\text{N}_2$  (496.60): C, 67.7; H, 7.31; N, 5.64. Found: C, 66.4; H, 7.18; N, 5.48.

**2,4-Bis[4-(*N,N*-diisobutylamino)-2,6-dihydroxyphenyl]squaraine (4).** Shining green-brown needle microcrystals, total yield: 23.9%. IR:  $\nu_{\max}$  3444, 3087, 2959, 2926, 2871, 2708, 1630 (C=O), 1550, 1498, 1430, 1402, 1349, 1322 (C–N), 1257 (OH), 1163, 1119, 1095, 961, 948, 926, 890, 870, 808, 797, 743  $\text{cm}^{-1}$ .  $^1\text{H}$  NMR ( $\text{CDCl}_3$ ):  $\delta$  10.963 (s, 4H, OH), 5.805 (s, 4H,  $\text{H}_{\text{arom}}$ ), 3.237 (d,  $J = 7.32$  Hz, 8H,  $\text{NCH}_2$ ), 2.124 (m, 4H,  $\text{NCH}_2\text{CH}$ ), 0.925 (d,  $J = 6.59$  Hz, 24H,  $\text{CH}_3$ ). MS (EI):  $m/z$  552 ( $\text{M}^+$ , 43.3%), 509 ( $\text{M}^+ - \text{C}_3\text{H}_7$ , 100%). Anal. Calcd for  $\text{C}_{32}\text{H}_{44}\text{O}_6\text{N}_2$  (552.70): C, 69.5; H, 8.02; N, 5.07. Found: C, 67.8; H, 7.97; N, 4.94.

**2.3. Langmuir Films.** A moving-wall LB-film deposition apparatus (Nippon Laser & Electronics Lab., NL-LB240-MWA) with a Wilhelmy balance was employed for the preparation of Langmuir films. Formation of Langmuir films of the SQ dye was achieved by spreading a 1,2-dichloroethane solution at a concentration of  $8.33 \times 10^{-4}$  mol/dm<sup>3</sup> (i.e., 20  $\mu\text{L} = 1 \times 10^{16}$  molecules) onto the pure water subphase of the trough with the water temperature maintained at 15 °C. In situ absorption spectra of the floating monolayers were obtained as a function of surface pressure by means of a fiber-optic multichannel photodiode array spectrometer (Otsuka Denshi, MCPD-100).

**2.4. Thermal Analysis.** The thermal stability of dyes 1–7 was investigated using a Shimadzu DTG-50 simultaneous DTA-TG measuring device. The measurements were carried out from room temperature to 500 °C in an atmosphere of argon gas with a flow rate of 30 mL/min, at a heating rate of 2 °C/min. Melting points and thermal decomposition temperatures were determined from the resulting DTA and TG curves.

**2.5. Evaluation of Sublimation Ability.** The sublimation ability of dyes 1–7 was evaluated through heating under vacuum. The SQ sample was put in a glass crucible, and the crucible was located at one end of a 60-cm-long, 3-cm-diameter transparent glass test tube. The tube was connected to an ULVAC VPC-250FA vacuum pump unit through a liquid nitrogen trap and evacuated to a vacuum lower than  $1 \times 10^{-3}$  Pa. Then, the sample was gradually heated under high vacuum using a tubular electric furnace. The thermal behavior of the sample was monitored during the heating process.

**2.6. Fabrication of SQ Thin Films by Molecular Beam Deposition.** Thin films of those sublimable SQ(OH)<sub>4</sub> dyes were prepared using an ULVAC BC4558 molecular beam epitaxy apparatus. The SQ sample was dispersed across the entire bottom of a quartz crucible and slowly heated in a K-cell under

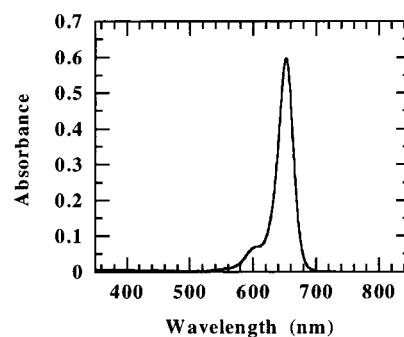


**Figure 2.** UV-visible absorption spectrum of dye 4 in 1,2-dichloroethane.

**TABLE 1: Absorption Properties of Dyes 1–7 in 1,2-Dichloroethane**

SQ dye	$\lambda_{\max}$ (nm)	$\epsilon$ (dm <sup>3</sup> mol <sup>-1</sup> cm <sup>-1</sup> )
1	644.0	$3.01 \times 10^5$
2	648.0	$3.45 \times 10^5$
3	651.0	$3.32 \times 10^5$
4	652.2	$3.20 \times 10^5$
5	649.2	$3.36 \times 10^5$
6	650.2	$3.39 \times 10^5$
7	650.6	$3.47 \times 10^5$

an ultrahigh vacuum of  $(0.2\text{--}2) \times 10^{-6}$  Pa. The dye film was evaporated onto a  $3 \times 3\text{-cm}^2$  glass substrate of 22 °C, and the deposition rate was monitored using a quartz crystal oscillator thickness meter. Heating temperature was controlled to give a deposition rate of 0.1–0.9 Å/s.

### 3. Results and Discussion

**3.1. Spectroscopic Properties in Solution.** Except for 1 and 2, SQ dyes 3–7 exhibit good solubility in halogenated solvents such as dichloromethane, 1,2-dichloroethane, and chloroform. The solution spectra of this class of SQ dyes are similar and, for example, in 1,2-dichloroethane have a sharp absorption band at approximately 650 nm with a well-defined shoulder at about 600 nm (Figure 2). This asymmetry is a familiar property of SQ dyes and may be attributed to aggregation, even at low concentrations.<sup>27</sup> The maximum absorption wavelengths ( $\lambda_{\max}$ ) and the molar extinction coefficients ( $\epsilon$ ) of dyes 1–7 in 1,2-dichloroethane are summarized in Table 1. It is noted that the order of  $\lambda_{\max}$  variation for these compounds is  $1 < 2 < 5 < 6 < 7 < 3 < 4$ . The reason for this phenomenon may be that the steric hindrance of *N*-alkyl causes the amino groups to rotate slightly or to vary in its ability to  $\text{sp}^2$  hybridize to participate in delocalization. We think that the larger steric hindrance effect of two neighboring *N*-alkyl chains conduces to the better participation of the amino groups in  $\pi$ -electron delocalization, resulting in the redshift of peak absorption. Since the steric hindrance of straight *N*-alkyl chain increases as the alkyl chain length grows, and branched *N*-alkyl chains such as *sec*-butyls and isobutyls have even larger steric hindrance than the straight ones, the  $\lambda_{\max}$  of the corresponding dyes will vary in the order as observed.

**3.2. Langmuir Films at the Air–Water Interface.** There is a report in the literature on the Langmuir films of dye 5 at the air–water interface.<sup>38</sup> Our investigation confirmed the earlier study of Ashwell et al.<sup>38</sup> As a representative result, the surface pressure–area ( $\pi$ – $A$ ) isotherms of dyes 2–5 and 7 are shown in Figure 3. Similar to the behavior of the *N*-methyl-*N*-alkyl analogues at the air–water interface,<sup>27</sup> the  $\pi$ – $A$  isotherms of this class of SQ dyes are generally featureless. The limiting areas for dyes 2–5 and 7, obtained by extrapolating the high-

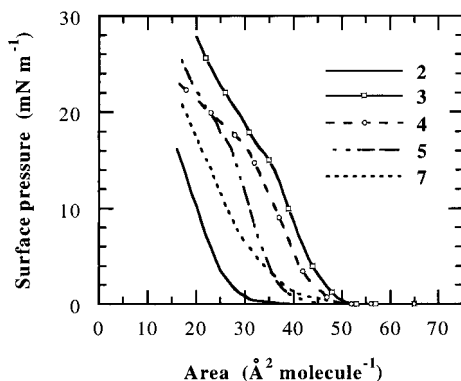


**Figure 3.** Surface pressure versus area isotherms of dyes 2–5 and 7 at ca. 15 °C.

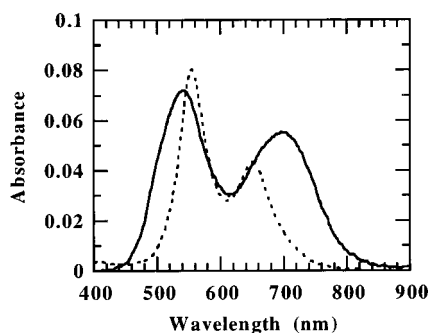


**Figure 4.** Typical absorption spectra of dyes 2 (solid line) and 7 (broken line) at the air–water interface for surface pressures of  $3 \leq \pi \leq 10 \text{ mN m}^{-1}$ .

pressure region of the isotherm to  $\pi = 0$ , are 28, 46.5, 45, 38, and  $40 \text{ \AA}^2 \text{ molecule}^{-1}$ , respectively. This result indicates that the longer straight *N*-alkyl chain has a larger steric hindrance than the shorter one, and the branched *N*-alkyl chains such as *sec*-butyls and isobutyls possess even larger steric hindrance than the straight ones, as we stated above. Since the van der Waals dimensions of the SQ chromophore, including the first methylene attached to each of the nitrogen atoms but without any hydroxyl group, are estimated to be ca.  $19 \text{ \AA}$  (length)  $\times$   $8 \text{ \AA}$  (width)  $\times$   $3.4 \text{ \AA}$  (thickness),<sup>27</sup> the limiting areas for dyes 1–7 are smaller than  $19 \text{ \AA}$  (length)  $\times$   $3.4 \text{ \AA}$  (thickness). This fact suggests that the SQ(OH)<sub>4</sub> molecules not only have very good coplanarity between the phenyl rings and the four-membered ring, but also exhibit a large intermolecular aggregation effect at the air–water interface. The good molecular planarity may be attributed to the intramolecular hydrogen bonding between the hydroxyls and the centric CO groups, and the large aggregation effect between SQ(OH)<sub>4</sub> molecules is believed to come from the intermolecular hydrogen bonding between the hydroxyls.

The absorption spectra of the Langmuir films at the air–water interface are dependent not only on the alkyl chain length but also on whether the alkyl chains are branched or not. The straight-chain analogues 1, 2, and 5–7 have a similar absorption type, i.e., main H-aggregate bands with maxima at ca. 540 nm and monomeric bands with maxima at 650–700 nm (Figure 4). The *N*-alkyl chain length has an influence on the maximum absorption position of the monomeric band. For example, dyes 5–7 have monomeric absorption bands with maxima at ca. 650 nm, whereas dyes 1 and 2 exhibit monomeric absorption bands with maxima at ca. 700 nm. On the other hand, the branched-butyl analogues 3 and 4 show a different absorption type, i.e., sharp J-aggregate bands with maxima at ca. 700–730 nm and a weak shoulder in the range of 550–660 nm (Figure 5). These

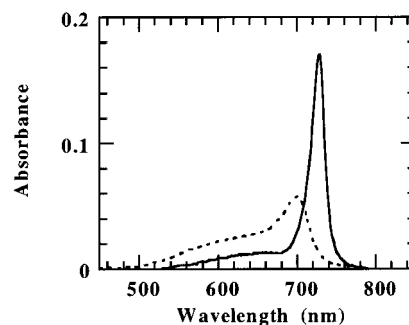


**Figure 5.** Typical absorption spectra of dyes 3 (solid line) and 4 (broken line) at the air–water interface for surface pressures of  $10 \leq \pi \leq 20 \text{ mN m}^{-1}$ .

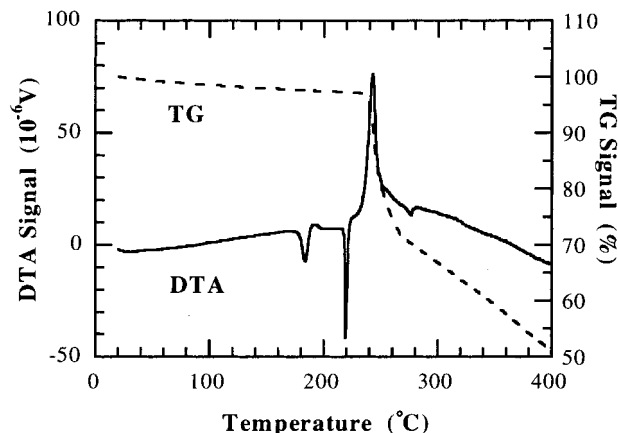


**Figure 6.** DTA-TG analysis curves for dye 3 ( $R^1 = n\text{-propyl}$ ,  $R^2 = \text{sec-butyl}$ ).

phenomena can be explained from the intermolecular interactions in the Langmuir films. In the case of the straight-chain analogues, we think that their monolayer structure is dominated by chromophore-induced interactions that consist mainly of the intermolecular hydrogen bonding between the aromatic hydroxyls. Since such intermolecular hydrogen bonding favors a parallel face-to-face arrangement of the chromophores, the formation of H-aggregates at the air–water interface will be markedly promoted.<sup>49</sup> Conversely, it is assumed that the van der Waals interactions between branched alkyl chains dictate the monolayer structure of the branched-alkyl analogues, and as a result, the strong steric hindrance effects stemming from branched butyls can suppress the intermolecular hydrogen bonding between the hydroxyls, and favor not the parallel face-to-face arrangement but the parallel face-to-breast alignment of the chromophores; therefore, the formation of J-aggregate in the Langmuir films will be significantly facilitated.<sup>49</sup> The behavior of the branched-butyl analogues 3 and 4 at the air–water interface demonstrated that the introduction of branched *N*-alkyls could provide sufficiently large intermolecular steric hindrance for the target SQ(OH)<sub>4</sub> molecules to overcome the intermolecular hydrogen bonding. In particular, because dye 3 has a slightly larger molecular limiting area than 4, and the Langmuir films of 3 show J-aggregate absorption bands at the longer wavelength side than of 4, we believe that the intermolecular steric hindrance of dye 3 is slightly larger than of 4.

**3.3. Thermal Stability.** Representative DTA-TG analysis curves for dyes 3 and 4 are shown in Figures 6 and 7, respectively. Dye 3 exhibited a crystal phase transition at 183.6 °C and a clear melting point at 219.2 °C. From the TG curve, its thermal decomposition temperature was found to be 237.0 °C. This result is consistent with the DTA analysis. Meanwhile,

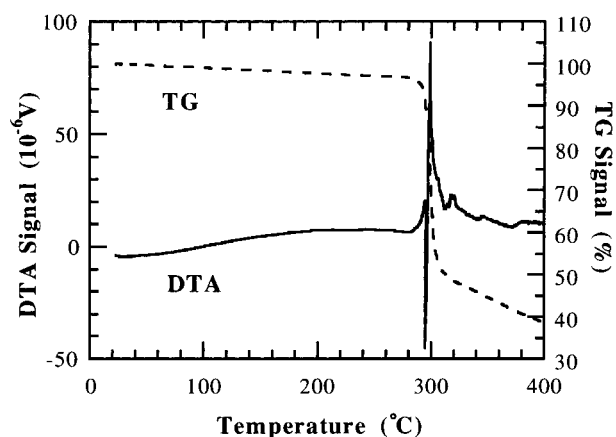


Figure 7. DTA-TG analysis curves for dye **4** ( $R^1 = R^2 =$  isobutyl).

TABLE 2: Melting Points and Thermal Decomposition Temperatures of Dyes 1–7

SQ dye	melting point (°C)	thermal decomp. temp. (°C)
<b>1</b>	>290	288.6
<b>2</b>	277.1	277.5
<b>3</b>	219.2	237.0
<b>4</b>	294.0	299.0
<b>5</b>	235.1	242.0
<b>6</b>	224.0	244.0
<b>7</b>	204.6	239.1

dye **4** melted at 294.0 °C and decomposed at 299.0 °C. The melting points and thermal decomposition temperatures of dyes **1–7** are given in Table 2. For the straight-chain analogues, both the melting points and the thermal decomposition temperatures decreased as the *N*-alkyl chain length increased. This phenomenon may be due to the influence of flexible *N*-alkyl chains. The longer straight *N*-alkyl chain has larger steric hindrance and hence would lead to less-compact spatial stacking of the corresponding SQ(OH)<sub>4</sub> molecules. Moreover, the longer *N*-alkyl chain will exhibit higher possibility to decompose on heating. These effects result in the decrease of the melting points and the thermal stability of the corresponding SQ(OH)<sub>4</sub> dyes with increasing chain length. However, for the branched-butyl analogues, their thermal behavior is slightly peculiar. Compound **3**, which has two *N*-*n*-propyls and two *N*-*sec*-butyls, shows a lower melting point and a lower thermal decomposition temperature than **2**, **5**, and **6**, which are substituted with four *n*-propyls, *n*-butyls, and *n*-pentyls, respectively. However, **4**, which has four *N*-isobutyls, exhibits the highest melting point and the highest thermal decomposition temperature among **2–7**. These phenomena may be due to the influence of the branching of *N*-alkyl chains. The branching position and the number of branching points determine the total influence of branched *N*-alkyl chains on the thermal properties of the corresponding SQ dye. The branching position closer to the phenyl ring would result in a larger steric hindrance and a higher possibility for the branched *N*-alkyl chain to decompose on heating. On the other hand, the number of branching points will influence the symmetry and spatial stacking of SQ molecules. Compound **3** has two *sec*-butyls, and the two branching points are directly connected to the nitrogen atoms. Such a molecular structure will result in three effects. The first one is that **3** will have lower molecular symmetry because of the possible free rotation of C–N bonds; thus, molecules of **3** have looser spatial stacking in the solid state. The second effect is that **3** will have the largest molecular free volume in the solid-state owing to the largest intermolecular steric hindrance, as revealed by its Langmuir films. The third effect is that the possibility for the *sec*-butyl

TABLE 3: Evaluation Results of the Sublimation Ability of Dyes 1–7<sup>a</sup>

SQ dye	initial sublim. temp. (°C)	initial decomp. temp. (°C)	sublim. compl. temp. (°C)
<b>1</b>	180	230	
<b>2</b>	180	260	260
<b>3</b>	150	220	220
<b>4</b>	170		250
<b>5</b>	170	230	
<b>6</b>	180	220	
<b>7</b>	190	220	

<sup>a</sup> The vacuum for sublimation experiments is  $(10\sim 4) \times 10^{-4}$  Pa.

chain to decompose on heating will be higher than those for short straight alkyl chains such as *n*-propyls and *n*-butyls. For these reasons, **3** shows a much lower melting point and a lower thermal decomposition temperature than **2**, **5**, and **6**. On the other hand, **4** has four branching points that are relatively far from the phenyl ring and symmetrically distributed at the two ends of the dye molecule. Such substitution reduces the possibility for the isobutyl chains to decompose on heating, and compared with **3**, **4** exhibits more-compact spatial stacking of molecules. Because **2** and **4–7** have the same molecular symmetry and the same backbone structure, in this case, it is assumed that their melting behavior is dominated by the flexibility of the four *N*-alkyl chains. Obviously, bulky isobutyl groups will have much lower flexibility than *n*-propyl, *n*-butyl, *n*-pentyl, and *n*-hexyl groups. Therefore, **4** will have much lower molecular flexibility than **2** and **5–7**. These may be the reasons why **4** shows a much higher melting point and a much higher thermal decomposition temperature than **2**, **3**, and **5–7**.

To further verify that an SQ(OH)<sub>4</sub> dye will show even better thermal stability than the corresponding dihydroxy analogue, we compare the thermal stability of 2,4-bis[4-(*N,N*-dipropylamino)-2-hydroxyphenyl]squaraine [SQ33(OH)<sub>2</sub>]<sup>50</sup> with that of **2**. The thermal decomposition temperatures of SQ33(OH)<sub>2</sub> and dye **2**, which were measured by DTA-TG analysis, are 226.0 and 277.5 °C, respectively. Apparently, dye **2** shows much higher thermal stability than SQ33(OH)<sub>2</sub>. Such a high thermal stability helps to improve the sublimation ability of the same dye molecules and hence is preferable for sublimable dyes.

**3.4. Sublimation Ability.** The evaluation results of the sublimation ability of SQ dyes **1–7** are summarized in Table 3. Dyes **1**, **6**, and **7** could be slightly sublimed under high vacuum when heated to 180, 180, and 190 °C, respectively, and on further heating, their sublimation rate increased very slowly, with most of their molecules decomposing before sublimation at higher temperatures. Dye **5** could be sublimed without decomposition at 170–230 °C under high vacuum, and its sublimation rate increased rapidly when it began to melt at 230 °C, owing to the significant improvement in the thermal conduction of the melting sample as compared with that of the unmelted sample powders. However, slight decomposition of its molecules also occurred at 230 °C. Similarly, dye **2** could be sublimed without decomposition at 180–260 °C under high vacuum, and its sublimation rate was sufficiently high at 250 °C to allow most of its molecules to evaporate. However, slight decomposition of its molecules also occurred at 260 °C. Regarding dye **3**, its sublimation started even at 150 °C under high vacuum, and the color of the sample at 190 °C changed from yellow-green to brown-green, and finally to golden brown, indicating the occurrence of a crystal phase transition. This compound could be well sublimed without decomposition at temperatures below 220 °C, and its sublimation rate increased rapidly when heated at a temperature near its melting point.

Most of this sample could be sublimed at 220 °C, although very slight decomposition of its molecules also occurred at 220 °C. In contrast, dye **4** could be well sublimed without decomposition from 170 °C under high vacuum, and its sublimation rate increased with heating temperature. We found that it was completely sublimed without any decomposition when heated to 250 °C, which was far lower than its melting point and thermal decomposition temperature.

It is necessary for us to explain what high sublimation ability means to a dye. Generally speaking, heating is required for a dye to be sublimed under vacuum. Thus, a dye with high sublimation ability should, first of all, be sufficiently thermally stable during the process of sublimation; i.e., its initial decomposition temperature should be higher than its initial sublimation temperature, and a larger difference between these two temperatures is preferable. Second, for such a dye, its sublimation rate should increase with heating temperature and be controllable. Moreover, it should be possible for such a dye to be sublimed completely far below its initial decomposition temperature. In fact, it is difficult to judge whether a dye has high sublimation ability without conducting practical sublimation experiments.

To verify the effectivity of our molecular design, the sublimation ability of SQ33(OH)<sub>2</sub> was also investigated for comparison. SQ33(OH)<sub>2</sub> could only be slightly sublimed when heated at 150 °C under high vacuum. On further heating, its sublimation rate increased very slowly, with most of its molecules decomposing before sublimation at temperatures higher than 180 °C. Undoubtedly, SQ33(OH)<sub>2</sub> exhibited a much worse sublimation ability than dye **2**. These results demonstrate that the four hydroxyls at the 2',6'-positions of the two phenyl rings enhance the sublimation ability of an anilino SQ dye molecule much more significantly than the two hydroxyls at the same 2'-positions. Furthermore, with the introduction of branched *N*-butyls, the target SQ(OH)<sub>4</sub> molecules can have sufficiently high sublimation ability for thin-film preparation under vacuum.

Some trends regarding the sublimation ability of these SQ dyes can be seen from Table 3. For the straight-chain analogues, the sublimation ability increases with the carbon number of the *N*-alkyl chain first, reaches a maximum at carbon numbers three and four, and then decreases again as the *N*-alkyl chain length increases further. Moreover, the two branched-butyl analogues show higher sublimation ability than the straight-chain ones, and dye **4** is the most sublimable material among these dyes. These phenomena can be explained from the inter- and intramolecular interactions of SQ molecules. The intramolecular hydrogen bonding between the hydroxyls and the centric CO groups greatly enhances both the thermal stability and the sublimation ability of the corresponding SQ(OH)<sub>4</sub> molecules to such an extent that the initial sublimation temperature is much lower than the thermal decomposition temperature. Thus, SQ dyes **1–7** were rendered sublimable. On the other hand, the *N*-alkyl chains have two influences on the intermolecular interactions. One is the attractive force between the alkyl chains, which grows with the chain length, and the other one is the repulsive force coming from the steric hindrance of the alkyl chains. The balance of these two forces determines the total influence of the *N*-alkyl chains on the sublimation ability of the SQ analogues. In general, the sublimation ability benefits from the intermolecular repulsive force. For the straight-chain analogues, the attractive force dominates when the alkyl chain has a carbon number less than three, while the repulsive force dominates as the carbon number of the alkyl chain increases to

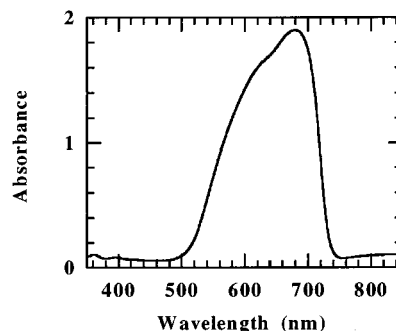


**Figure 8.** UV-visible absorption spectrum of a 57.5-nm-thick, molecular-beam-deposited film of dye **4**.

three and four. After that, the attractive force between the alkyl chains dominates again as the alkyl chain length increases further. This is why dyes **2** and **5** exhibit the maximum sublimation ability among the straight-chain analogues. Moreover, when branched butyls replace the straight alkyl chains, the additional steric hindrance caused by the branching of butyls enhances the intermolecular repulsive force and suppresses the intermolecular hydrogen bonding between the hydroxyls, as demonstrated in the Langmuir films of these SQ(OH)<sub>4</sub> dyes. Thus, the sublimation ability of the corresponding SQ dye increases. This is why dyes **3** and **4** show lower temperatures of initial sublimation than the other SQ(OH)<sub>4</sub> dyes. In addition, although dye **4** has a much higher melting point, its sublimation ability depends mainly on the intermolecular repulsive interactions. Since the presence of four bulky isobutyls would result in the largest intermolecular repulsive force, dye **4** exhibits the highest sublimation ability among all the seven compounds. These results suggest that an SQ(OH)<sub>4</sub> molecule with branched *N*-butyls is the most effective structure for realizing a high sublimation ability. Although we have not succeeded in the preparation of SQ(OH)<sub>4</sub> molecules with four *N*-*sec*-butyls or *N*-*tert*-butyls, or with a combination of isobutyl, *sec*-butyl, and *tert*-butyl groups at the nitrogen atoms, these molecules can also be expected to show even higher sublimation ability.

**3.5. Molecular-beam-deposited Films.** Since only dye **4** could be completely sublimed without any decomposition, this dye was employed for thin-film fabrication under vacuum. Pure thin films of dye **4** were successfully fabricated by molecular beam deposition at a rate of 0.1–0.8 Å/s when the sample was heated at 245 °C under an ultrahigh vacuum of  $(0.3–2) \times 10^{-6}$  Pa. The UV–visible absorption spectrum of such a film with a thickness of 57.5 nm is shown in Figure 8. The molecular-beam-deposited (MBD) film of dye **4** exhibited a broad absorption band with the peak located at 680 nm. Compared to the absorption of its solution, the absorption of the MBD film is redshifted by 28 nm. This indicates that J-like aggregates were formed in the MBD films. Such aggregates are very important for application in nonlinear optics.<sup>17,31,32</sup> The behavior of dye **4** in the MBD films is similar to that in its monolayers at the air–water interface. Because MBD films have higher surface flatness and better thickness homogeneity than solution-coated films, and their thicknesses are precisely controllable, such thin films of sublimable SQ dyes such as **4** are indispensable for fabricating many optical and electrooptic devices containing SQ films.

#### 4. Conclusions

As an effort to obtain sublimable SQ materials superior to known SQ dyes, we have synthesized a series of tetrahydroxy anilino SQ derivatives, SQ(OH)<sub>4</sub> dyes **1–7** and studied their

properties. The behaviors of their Langmuir films at the air–water interface demonstrate that the longer straight *N*-alkyl chain has a larger steric hindrance than the shorter one, and the branched *N*-alkyl chains such as *sec*-butyls and isobutyls possess even larger steric hindrance than the straight ones. It is also manifested that the intermolecular hydrogen bonding between the aromatic hydroxyls favors the formation of SQ(OH)<sub>4</sub> H-aggregates at the air–water interface. However, the branching of *N*-alkyl chains greatly suppresses the formation of H-aggregates and facilitates the formation of J-aggregates in the Langmuir films, owing to the strong steric hindrance of the bulky branched *N*-alkyls. The evaluation of the monolayers at the air–water interface proved effective in assessing intermolecular interactions, especially intermolecular steric hindrance. Moreover, from investigations of dyes **1–7** by DTA and TG, as well as by heating under vacuum, we demonstrated that the four hydroxyls at the 2',6'-positions of the two phenyl rings enhanced the thermal stability and the sublimation ability of an anilino SQ dye molecule much more significantly than the two hydroxyls at the same 2'-positions, and the introduction of branched *N*-butyls further lowered the sublimation temperatures of the target SQ(OH)<sub>4</sub> molecules. It was also clarified that the intramolecular hydrogen bonding between the hydroxyls and the centric CO groups, and the branching of *N*-alkyl chains can greatly enhance the sublimation ability of the corresponding SQ(OH)<sub>4</sub> molecules, whereas the intermolecular hydrogen bonding between the hydroxyls should be suppressed to improve their sublimation ability. In particular, dye **4**, which has four *N*-isobutyls, exhibited excellent sublimation ability and could be sublimed without any decomposition. Furthermore, pure SQ dye thin films that have been obtained only by solution coating so far were successfully fabricated by molecular beam deposition of dye **4**. Similar to the behavior in the Langmuir films at the air–water interface, not H-aggregates but J-like aggregates were formed in the MBD thin films of dye **4**. Such thin films of SQ dyes may find technological applications in many areas such as electrophotography, solar energy conversion, optical recording, and nonlinear optics.

**Acknowledgment.** The New Energy and Industrial Technology Development Organization (NEDO) supported this work within the framework of the Femtosecond Technology Research Project.

## References and Notes

- Meiz, R. J.; Champ, R. B.; Chang, L. S.; Chiou, C.; Keller, G. S.; Liclian, L. C.; Neiman, R. B.; Shattuck, M. D.; Weiche, W. J. *Photogr. Sci. Eng.* **1977**, *21*, 73.
- Tam, A. C. *Appl. Phys. Lett.* **1980**, *37*, 979.
- Law, K. Y. *Chem. Rev.* **1993**, *93*, 449.
- Merritt, V. Y.; Hovel, H. J. *Appl. Phys. Lett.* **1976**, *29*, 414.
- Merritt, V. Y. *IBM J. Res. Dev.* **1978**, *22*, 353.
- Musser, M. E.; Dahlberg, S. C. *Appl. Surface Sci.* **1980**, *5*, 28.
- Yamin, P.; Piechowski, A. P.; Bird, G. R.; Morel, D. L. *J. Phys. Chem.* **1982**, *86*, 3796.
- Jipson, V. B.; Jones, C. R. *IBM Technol. Disclosure Bull.* **1981**, *24*, 298.
- Gravesteyn, D. J.; Steenbergen, C.; van der Ween, J. *Proc. SPIE-Int. Soc. Opt. Eng.* **1983**, *420*, 327.
- Sporer, A. H. *Appl. Optics* **1984**, *23*, 2738.
- Dirk, C. W.; Kuzyk, M. G. *Chem. Mater.* **1990**, *2*, 4.
- Zu, Y. Z.; Shi, R. F.; Garito, A. F.; Grossman, C. H. *Opt. Lett.* **1994**, *19*, 786.
- Andrews, J. H.; Khaydarov, J. D. V.; Singer, K. D. *Opt. Lett.* **1994**, *19*, 984.
- Dirk, C. W.; Herndon, W. C.; Cervantes-Lee, F.; Selnau, H.; Martinez, S.; Kalamegham, P.; Tan, A.; Campos, G.; Velez, M.; Zyss, J.; Ledoux, I.; Cheng, L.-T. *J. Am. Chem. Soc.* **1995**, *117*, 2214.
- Ashwell, G. J.; Jefferies, G.; Hamilton, D. G.; Lynch, D. E.; Roberts, M. P. S.; Bahra, G. S.; Brown, C. R. *Nature* **1995**, *375*, 385.
- Ashwell, G. J. *Adv. Mater.* **1996**, *8*, 248.
- Furuki, M.; Pu, L. S.; Sasaki, F.; Kobayashi, S.; Tani, T. *Appl. Phys. Lett.* **1998**, *21*, 2648.
- Mori, T.; Miyachi, K.; Kichimi, T.; Mizutani, T. *Jpn. J. Appl. Phys.* **1994**, *33*, 6594.
- Zhang, B.; Zhao, W.; Cao, Y.; Wang, X.; Zhang, Z.; Jiang, X.; Xu, S. *Synth. Met.* **1997**, *91*, 237.
- Swalen, J. D.; Tacke, M.; Santo, R.; Rieckhoff, K. E.; Fisher, J. *Helv. Chem. Acta* **1978**, *61*, 960.
- Kawabata, Y.; Sekiguti, T.; Tanaka, T.; Nakamura, T.; Koizumi, H.; Honda, K.; Manda, E.; Saito, M.; Sugi, M.; Iizima, S. *J. Am. Chem. Soc.* **1985**, *107*, 5270.
- Kim, S.; Furuki, M.; Pu, L. S.; Nakahara, H.; Fukuda, K. *J. Chem. Soc., Chem. Commun.* **1987**, 1201.
- Kim, S.; Furuki, M.; Pu, L. S.; Nakahara, H.; Fukuda, K. *Thin Solid Films* **1988**, *159*, 1201.
- Law, K. Y.; Chen, C. C. *J. Phys. Chem.* **1989**, *93*, 2533.
- Liang, K.; Law, K. Y.; Whitten, D. G. *J. Phys. Chem.* **1994**, *98*, 13379.
- Ashwell, G. J.; Wong, G. M. S.; Bucknall, D. G.; Bahra, G. S.; Brown, C. R. *Langmuir* **1997**, *13*, 1629.
- Ashwell, G. J.; Jefferies, G.; Rees, N. D.; Williamson, P. C.; Bahra, G. S.; Brown, C. R. *Langmuir* **1998**, *14*, 2850.
- Loutfy, R. O.; Hsiao, C. K.; Kazmaier, P. M. *Photogr. Sci. Eng.* **1983**, *27*, 5.
- DiPaola-Baranyi, G.; Hsiao, C. K.; Kazmaier, P. M.; Burt, R.; Loutfy, R. O.; Martin, T. I. *J. Imaging Sci.* **1988**, *32*, 60.
- Law, K. Y. *J. Imaging Sci.* **1990**, *34*, 38.
- Tatsuura, S.; Furuki, M.; Tian, M.; Sato, Y.; Pu, L. S. *Mater. Res. Soc. Symp. Proc.* **1999**, *561*, 105.
- Tatsuura, S.; Tian, M.; Furuki, M.; Sato, Y.; Pu, L. S.; Wada, O. *Jpn. J. Appl. Phys.* **2000**, *39*, 4782.
- Baranyi, G.; Burt, R. A.; Hsiao, C. K.; Kazmaier, P. M.; Carmichael, K. M.; Horgan, A. M. U. S. Patent 4,471,041, 1984.
- Kazmaier, P. M.; Burt, R.; DiPaola-Baranyi, G.; Hsiao, C. K.; Loutfy, R. O.; Martin, T. I.; Hamer, G. K.; Bluhm, T. L.; Taylor, M. G. *J. Imaging Sci.* **1988**, *32*, 1.
- Garvey, D. W.; Zimmerman, K.; Young, P.; Tostenrude, J.; Townsend, J. S.; Zhou, Z.; Lobel, M.; Dayton, M.; Wittorf, R.; Kuzyk, M. G.; Sounick, J.; Dirk, C. W. *J. Opt. Soc. Am. B* **1996**, *13*, 2017.
- Mathis, K. S.; Kuzyk, M. G.; Dirk, C. W.; Tan, A.; Martinez, S.; Gampos, G. *J. Opt. Soc. Am. B* **1998**, *15*, 871.
- Kuzyk, M. G.; Garvey, D. W.; Vigil, S. R.; Welker, D. J. *Chem. Phys.* **1999**, *245*, 533.
- Ashwell, G. J.; Williamson, P. C.; Green, A.; Bahra, G. S.; Brown, C. R. *Aust. J. Chem.* **1998**, *51*, 599.
- Zhong, T. X.; Workman, R. K.; Yao, X.; Jabbour, G. E.; Peterson, C. A.; Sarid, D.; Dirk, C. W.; de la Cruz, D.; Nagarur, A. *Thin Solid Films* **1998**, *315*, 294.
- Yang, M.; Jian, Y. *Phys. Chem. Chem. Phys.* **2001**, *3*, 4213.
- Kruhlak, R. J.; Young, J.; Kuzyk, M. G. *Proc. SPIE-Int. Soc. Opt. Eng.* **1997**, *3147*, 118.
- Kruhlak, R. J.; Kuzyk, M. G. *Proc. SPIE-Int. Soc. Opt. Eng.* **1998**, *3473*, 57.
- Kruhlak, R. J.; Kuzyk, M. G. *J. Opt. Soc. Am. B* **1999**, *16*, 1749.
- Kruhlak, R. J.; Kuzyk, M. G. *J. Opt. Soc. Am. B* **1999**, *16*, 1756.
- Garvey, D. W.; Kuzyk, M. G. *Proc. SPIE-Int. Soc. Opt. Eng.* **1999**, *3796*, 13.
- Ashwell, G. J. *J. Mater. Chem.* **1998**, *8*, 373.
- Meier, H.; Petermann, R.; Gerold, J. *Chem. Commun.* **1999**, 977.
- Sprenger, H. E.; Ziegenbein, W. *Angew. Chem., Int. Ed. Engl.* **1966**, *5*, 894.
- McRae, E. G.; Kasha, M. *J. Chem. Phys.* **1958**, *28*, 721.
- Law, K. Y. *J. Phys. Chem.* **1987**, *91*, 5184.